Astron. Astrophys. 315, L60–L63 (1996)

ASTRONOMY
AND
ASTROPHYSICS

The wavelength calibration and resolution of the SWS⋆

E.A. Valentijn[1,3], H. Feuchtgruber[2,3], D.J.M. Kester[1], P.R. Roelfsema[1,3], P. Barr[3], O.H. Bauer[2], D.A. Beintema[1,3], D.R. Boxhoorn[1,3], Th. de Graauw[1], L.N. Haser[2], A. Heske[3], A.M. Heras[3], R.O. Katterloher[2], F. Lahuis[1,3], D. Lutz[2], K.J. Leech[3], P.W. Morris[3,5], A. Salama[3], S.G. Schaeidt[2,3], H.W.W. Spoon[2,5], B. Vandenbussche[3,4], E. Wieprecht[2,3] W. Luinge[1], and K.J. Wildeman[1]

[1] SRON, P.O. Box 800, 9700 AV Groningen, The Netherlands
[2] Max-Planck-Institut für extraterrestrische Physik, Postfach 1603, D-85740 Garching, Germany
[3] ISO Science Operations Centre, Astrophysics Division of ESA, P.O. Box 50727, E-28080 Villafranca/Madrid, Spain
[4] Institute for Astronomy, University of Leuven, B-3001 Heverlee, Belgium
[5] SRON, Sorbonnelaan 2, 3584 CA Utrecht, The Netherlands

Received 1 August 1996 / Accepted 18 September 1996

Abstract. The laboratory wavelength calibration of the SWS has been succesfully transferred to the in orbit situation. The achieved accuracies for the grating sections are $\lambda/\delta\lambda \sim 10000$. Any remaining errors in the wavelength scale are dominated by uncertainties of the relative position of the target in the $14''-20''$ wide slits. The grating spectral profile is very well represented by a Gaussian shape. The width of the grating spectral profile can be accurately predicted by a theoretical model. The wavelength calibration of the FP's is accurate to within 1/3 of a resolution element, corresponding to $\lambda/\delta\lambda \sim 10^5$. The wavelength stability of the gratings and FP is excellent, no measurable changes were found during the first 6 months of the ISO mission.

Key words: wavelength calibration, spectral resolution, infrared spectroscopy

1. Introduction

This letter describes the in-orbit wavelength calibration and spectral resolving power of ISO's short wavelength spectrometer (SWS). For an overview of ISO see Kessler et al. (1996). For the instrument, its observing modes and data reduction techniques see de Graauw et al (1996). The photometric calibration is described in Schaeidt et al (1996).

Pre-flight the wavelength calibration of the two grating sections and the two Fabry-Perot (FP) channels was characterised during a series of Instrument Level Tests (ILT). Reports on these can be found in Valentijn et al. (1993) and Beintema et al. (1993). In these measurements H_2O, NH_3 and HCl vapour cells and a set of lasers at 4, 10, 16 and 28 μm were used as SWS input sources to obtain wavelength calibration data. Analysis of these data resulted in a set of tables and constants defining accurately the relation between wavelength and scanner angle for the 3 aperture slits and the 6 detector arrays.

During the ILT's also the internal SWS wavelength calibration sources were used. Two for each grating section, positioned next to the entrance apertures, and one for the FP's. For the grating sections these sources consist of a hot element with a fixed FP, producing a series of fringes. The wavelengths of these fringes were calibrated using the vapour source calibration taking into account a correction needed for the off-aperture location of the internal sources.

In-orbit, first the internal wavelength calibration sources were measured again, to check for possible changes due to launch vibration effects and the new situation of zero-gravity. From this measurement a first order correction to the pre-flight wavelength calibration was derived. To establish the final wavelength calibration accuracy a number of well known emission lines of Planetary Nebulae (PN) are observed. Several of these lines in the LW section have an improved wavelength determination by observations with the FP (see Table 1).

For the FP's the situation is different. Here the internal wavelength calibration source is a fixed, stable FP, providing a series of very narrow transmission peaks. The in-orbit wavelength calibration of the two FP's relies mainly on the ground calibration of these peaks which is assumed to be unchanged in-orbit. Line observations towards astronomical sources are used for confirmation only.

Send offprint requests to: E.A. Valentijn

⋆ ISO is an ESA project with instruments funded by ESA Member States (especially the PI countries: France Germany, the Netherlands and the United Kingdom) and with the participation of ISAS and NASA.

SWS is a joint project of SRON and MPE (DARA grants no 50 QI9402 3 and 50 QI8610 8) with contributions from KU Leuven, Steward Observatory, and Phillips Laboratory.

Table 1. Lines used for the grating wavelength calibration

SW section			LW section		
Ion	Wavelength [μm]	Ref.	Ion	Wavelength [μm]	Ref.
[Mg IV]	4.488	a	[Ne II]	12.81355	b
[Ar VI]	4.527	a	[Mg V]	13.5213	d
[Mg V]	5.608	a	[Ar V]	13.1022	d
[Ar II]	6.98527	b	[Ne III]	15.5551	d
[Ar III]	8.99103	c	[S III]	18.7125	c
[Si IV]	10.5105	a	[Ne V]	24.3175	d
H recombination lines			[O IV]	25.8903	d
			[S III]	33.4810	d
			[Ne III]	36.0135	d

[a] Schmid-Burgk 1982, [b] Yamada et al. 1985,
[c] Kelly & Lacy 1995, [d] From FP observations

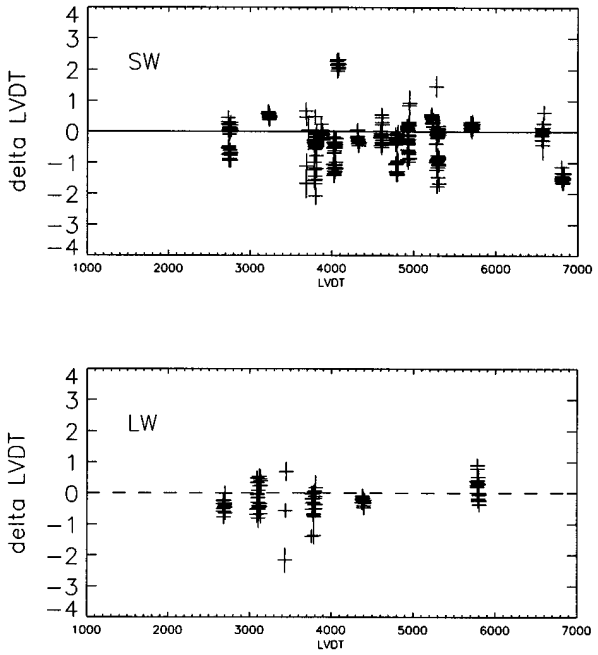

Fig. 1. Example residuals of the wavelength calibration in instrumental units LVDT from observations of Planetary Nebulae. Top figure: SW grating section using H recombination lines in NGC 7027, and ionic lines in IC 2501, Bottom figure: LW grating section, using ionic lines in IC 2501 (for wavelengths see Table 1).

As the LW grating section serves as order filter for the scanning FP's and as the free spectral range of the FP's is close to the grating spectral resolution, the wavelength calibration of the LW grating is critical for the FP *operation* and has to be carried out first. However, it does not affect the FP wavelength *calibration*.

The spectral resolution and instrumental profile have been determined during the ILT's with the vapour sources and laser emission lines filling the slit apertures. Therefore, in-orbit line observations provide the first opportunity to determine these instrument characteristics for a point source.

2. Grating wavelength calibration

For each grating section, rotating scan mirrors are used to vary the angle of incidence onto the gratings (see Wildeman et al 1987, Aalders et al. 1988). The relation between the incident angles and the resulting reflected wavelength λ is given by the grating equation:

$$\lambda N/D = \sin(\theta + \beta) + \sin(\theta + \delta) \quad (1)$$

Here N is the grating order, D is the grating constant; θ is the angle of the scan mirror, β is the offset angle of the beam from the aperture used and δ is the offset angle of the beam towards the detector. The angle of the scan mirror is measured by a Linear Voltage Differential Transducer (LVDT). As a first approximation the relation between scan angle and LVDT reading is well represented by a linear relation. However, the high wavelength calibration accuracy requires detailed modelling of the non-linear residuals in the θ-LVDT relation. It was found from the ILT calibration that this relation can be adequately described by a fifth order polynomial function. All together 18 constants are needed to be determined for a full description of the wavelength calibration: 6 for the polynome, 3 for the aperture offsets, 6 for the detector arrays and 3 for the offset angles to the grating and FP wavelength calibration sources. The offset angles to the detector bands were described for each array with an offset to the first array elements plus a constant pitch value between the elements. During the ILT's these two values were determined for each array using the laser lines. The offset of aperture 3 and of detector arrays 2 and 4 are defined as being 0 as these components were considered to be close to the optical axis of the instrument.

The fixed FP filters of the grating wavelength calibration have an effective thickness dr (thickness $\times$ refractive index) of 1101.7 and 822.26 μm for the SW and the LW sections respectively. As dr was found to vary significantly with wavelength from 2.5 to 45 μm the theoretical fringe wavelengths could not be used for the wavelength calibration. However, by analysing the periodicity the effective thickness could be estimated. The exact grating constants and all other constants needed for the wavelength calibration were also derived from the ILT data.

For the in-orbit calibration the following measurements and observations were made:

- Full scans of the grating wavelength calibration source. The measured LVDT values of the fringe peaks were used to update the LVDT-θ relation. The difference between the preflight and in-flight calibration was mainly a zeropoint shift, 25 LVDT units for the SW section and 10 for the LW. 1 LVDT unit is about 1/8 resolution element or 13.4″ in θ.
- Scans of selected lines in the planetary nebulae NGC 6543, NGC 7027, IC 2501, NGC 3918 and NGC 6826. All but IC 2501 are extended for the SWS. As most of the PNs fill the

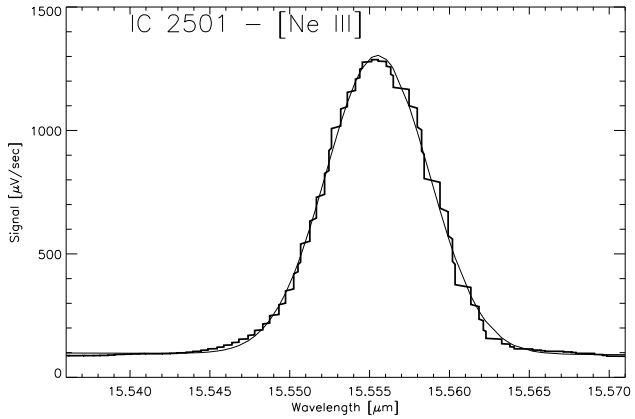

Fig. 2. [Ne III] 15.5551 μm line observed in the compact PN IC 2501. The Gaussian fit has a FWHM corresponding to R =2047. Our model predicts R = 2004 for a point source.

slit, pointing errors have become irrelevant for the wavelength calibration. These data were used to further update the angles. For the LW section these additional corrections are 11″ (equivalent to 0.8 LVDT) for the wavelength calibration source angle and 4″ (= 0.3 LVDT) for aperture 1; for the SW section, 87″ (= 6.5 LVDT) for detector band 1.

– Observations towards η Car with the FP in a fixed position and the grating scanning. With the wavelength calibration of the FP for the peaks of the fringes from the strong continuum we could update the wavelength calibration for wavelength above 35 μm where suitable emission lines in PN are lacking. Also here we rely on the (groundbased) calibration of the FP.

Fig. 1 shows residuals of the measured wavelengths of lines in IC 2501 versus the reference wavelengths after the calibration was updated. For the LW section the differences show an accuracy of 0.5-1 LVDT. For the SW section this is 1 LVDT. These values correspond to 1/10–1/5 of a resolution element.

While for the LW section we believe we have achieved optimal accuracy, constrained by the stepping of the scan mirror and the physical dimensions of the detectors, for the SW section a small improvement might be still possible. In practice however, errors probably are dominated by uncertainties of the relative position of the target in the $14'' - 20''$ wide slits. For a point source offset by 4″ from the center of the slit this results in an error in the wavelength scale corresponding to 1 LVDT.

Since launch, up to revolution 230 the scanners showed excellent stability, within 0.2 LVDT.

3. Grating Spectral Resolution

The instrumental profiles (IP) of the two grating sections were characterised during the ILT with the laser and vapour sources uniformly illuminating the entire apertures. In orbit strong emission lines of the pointlike source IC 2501 were used to determine the IP's of both grating sections at a number of wavelengths. The IP's are all very close to Gaussian over the entire wavelength range, down to 10 % of the peak level (see Fig. 2 for a typical example at 15.5 μm). They show no variation for different detector elements of a single array or at a different location along the slit. The FWHM of the IP varies substantially over the SWS wavelength range. The measured values are plotted in Fig. 3 together with the model calculations and show an excellent agreement to within a few percent. The impact of memory effects and pointing stability on the IP is less than expected pre-launch.

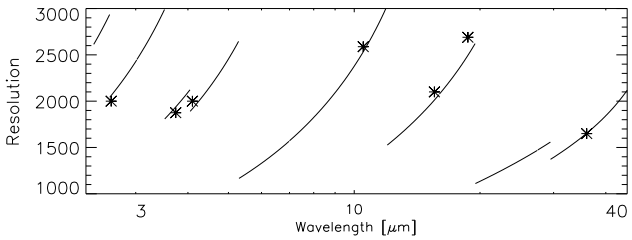

Fig. 3. The theoretical spectral resolution of both the SW and the LW section of the SWS, see text. The asterisks represent observed values from lines detected in the compact (nearly point source) Planetary Nebula IC 2501.

Table 2. Observed external wavelength standards for the FP wavelength calibration

Line	Vac. Wavelength [μm]	Meas. Offset [μm]	Object.
[Ne II]	12.81355±(2)[a]	+(4)	NGC7027
[Mg V]	13.52120±(2)[b]	−(6)	NGC7027
H_2 S(1)	17.034835±(6)[c]	−(60)	Saturn
H_2 S(1)	17.034835±(6)[c]	+(50)	Jupiter
H_2 S(0)	28.21883±(2)[c]	−(5)	Saturn
H_2 S(0)	28.21883±(2)[c]	+(9)	Jupiter
H_2O	29.83671±(1)[d]	−(18)	W Hya
H_2O	31.77205±(1)[d]	+(2)	W Hya
HD R(2)	37.70154±(1)[e]	−(1)	Jupiter
HD R(2)	37.70154±(1)[e]	+(20)	Saturn
H_2O	40.69087±(1)[d]	−(21)	W Hya

Numbers in brackets relate to last decimals
[a] Yamada et al. 1985, [b] Kelly & Lacy 1995
[c] Jennings et al. 1987, [d] HITRAN [e] Ulivi et al. 1991

4. Fabry-Perot Wavelength Calibration

The SWS FP calibration source with a fixed FP and twice the thickness of the scanning FP provides a very fine grid of narrow transmission peaks around 25 μm. The wavelengths of these transmission peaks were accurately determined (0.001 cm^{-1}) at LHe temperature using a Fourier Transform Spectrometer (FTS). A few of these peaks were first used for the automatic parallelisation procedure which uses the on board computer and adjusts the plates holding the mesh by maximising the peak in-

Table 3. SWS Fabry-Perot spectral resolution limits

Line	H_2	H_2O	H_2O
λ [μm]	17.0348	29.8367	40.6909
$\lambda/\delta\lambda$ FWHM	>25000	>30000	>30000

tensities. A large number of the transmission peaks was subsequently used to determine the actual gap of the FP and to linearise the gap-position relation. After analysis of these data the on-board drive current lookup table could be updated. For details about the FP drive see Beintema et al. (1993).

The accuracy of the internal wavelength calibration was, as expected, about 1 FP scanner step at 24 μm, which corresponds to about $10^{-4}\mu$m. However, the effective FP gap is slightly dependent on wavelength, because shorter wavelengths penetrate deeper into the reflecting meshes. During the ILT's, vapour absorption lines were measured to determine this gap correction, which has a maximum of about one FP resolution element over the full wavelength range of the FPs. Remaining uncertainties of this correction and the memory effects of the Si:Sb detector material used in the shortwave FP section cause a final uncertainty in the wavelength calibration of 2 FP scanner steps between 11.4 μm and 26 μm and 1 FP scanner step between 26 μm and 44.5 μm. Regular checks of the internal calibration during PV and routine phase indicate excellent stability over a period of 6 months.

The verification of the wavelength calibration by observations of external spectral lines suffers from the lack of accurate wavelength standards and radial velocities. However, a few lines (see Table 2) could be used to verify the internal calibration and the resulting accuracy is 1/3 of a resolution element or better. It is expected that the wavelength accuracy will improve slightly when more lines are observed.

5. Fabry-Perot Instrumental Profile

The FP instrumental profile is determined by scanning the internal calibrator lines. The result is the convolution of the Lorentz profile of the fixed FP and the Lorentz profile of the scanning FP. As the thickness ratio of the two FPs is known (1:2.3) the FWHM of the scanning FP instrumental profile can be recalculated. The FWHM resolutions found are R = 41900 $\pm$ 7000 at 24.61 μm and R = 29900 $\pm$ 3600 at 24.78 μm for the SW and the LW FP respectively. The errors are caused by the actual uncertainty of the FWHM of the fixed FP which could not be resolved by the FTS.

The instrumental profile on external sources is difficult to characterise, because no strong, sufficiently narrow, lines have been found up to now. However, the few lines measured with intrinsic widths of less or equal 10-15 km/s provide lower limits of the FP resolution at the respective wavelengths (see Table 3).

6. Conclusions

The wavelength calibration and the spectral resolution of the grating and the FP sections of the SWS have been characterised in orbit and achieved the required performance. For the SW section $\lambda/\delta\lambda$ varies between 5000 and 12000, for the LW section between 16000 and 8000, and for the FP $\lambda/\delta\lambda \sim 10^5$. The achieved accuracies already allowed to improve the rest wavenumbers of 29 ionic lines used in ISO observations (Feuchtgruber et al. 1996).

References

Aalders, J.W.G. et al. Cryogenics (1989) 550-552

Beintema D. et al., 1993, SPIE Conference Orlando USA, *Infrared Detectors and Instrumentation*, Vol. 1946, p. 293

Feuchtgruber H. et al., 1996, in this issue

de Graauw, Th. et al., 1996 in this issue

Hucht van der K. A., Lutz D., 1994, *ISO Short Wavelength Spectrometer Observer's Manual*, issue 2.0, ESA

Jennings D. E., Weber D. E., Brault J. W., 1987, J. Mol. Spectr. 126, 19

Kelly D. M., Lacy J. H., 1995, ApJ, 454, L161-L164

Kessler, M.F. et al., 1996 in this issue

Rothman L. S. et al. 1992, *The HITRAN Molecular Database* , J. Quant. Spectrosc. Radiat. Transfer Vol. 48, 5/6, 469-507

Schaeidt, S.G. et al., 1996 in this issue

Schmid-Burgk, J., 1982, in: Landolt-Boernstein, Neue Serie, 2c, 115.

Ulivi L., De Natale P., Inguiscio P., 1991, ApJ 378,L29

Valentijn, E.A et al., 1993, SPIE Conference No 2019, Infrared Technology, San Diego, USA

Wildeman, K.J. et al., 1987, Cryogenics 27 68-72

Yamada C., Kanamori H., Hirota E., 1985, J. chem. Phys., 83, 552